

COMPARATIVE ISOCONVERSIONAL THERMAL ANALYSIS AND DEGRADATION KINETICS OF *SALVIA SPINOSA* (KANOKHA) SEED HYDROGEL AND ITS ACETATES: A POTENTIAL MATRIX FOR SUSTAINED DRUG RELEASE

ARSHAD ALI,* MUHAMMAD AJAZ HUSSAIN,* AZHAR ABBAS,* TASKIN AMAN KHAN,*
GULZAR MUHAMMAD,** MUHAMMAD TAHIR HASEEB*** and IRFAN AZHAR****

*Institute of Chemistry, University of Sargodha, Sargodha 40100, Pakistan

**Department of Chemistry, Government College University, Lahore 54000, Pakistan

***College of Pharmacy, University of Sargodha, Sargodha 40100, Pakistan

****Key Laboratory of Nanobiosensing and Nanobioanalysis, Department of Chemistry, Northeast Normal University, 5268 Renmin Str., Changchun, Jilin Province, 130024, China

✉ Corresponding author: M. A. Hussain, majaz172@yahoo.com

Received October 8, 2021

The present study deals with the isolation and modification of *Salvia spinosa* hydrogel (SSH) to investigate its thermal degradation profile. The SSH was modified chemically to its acetylated derivative (ASSH-1–4) with DS 1.05–2.79. After characterization by Fourier transform infrared (FTIR) and solid-state CP/MAS ¹³C-NMR spectroscopic techniques, both SSH and ASSH-4 were subjected to thermogravimetric analyses (TG) by the isoconversional method, *i.e.*, the Flynn-Waal-Ozawa (FWO) and the Kissinger methods. TG curves showed that both SSH and ASSH-4 exhibited two-step degradation. The energy of activation (E_a) for each degradation step was calculated by fitting thermal degradation data to the FWO method, revealing greater stability of ASSH-4 than that of SSH. Analysis by Kissinger's method revealed the second and one and a half order of thermal degradation (n) for SSH and ASSH-4, which also evidenced that ASSH-4 is more stable than SSH. The values of the thermodynamic triplet (ΔH , ΔG and ΔS) were calculated from thermal data. Positive values were found for ΔG , which showed the non-spontaneous nature of thermal degradation of SSH and ASSH-4. The values of integral procedural decomposition temperature (IPDT) and intrinsic thermal stability (ITS) for SSH and ASSH-4 were found comparatively greater than those of many other commercially available materials of the same kind, which revealed the higher stability of both materials. SSH, as a benign polysaccharide-based material, was also assessed for its utility in drug release studies, taking caffeine as a model drug. The SSH matrix-based tablet formulation (SSHC) showed a sustained release behavior of the drug in preliminary studies.

Keywords: *Salvia spinosa* hydrogel, polysaccharides, acetylation, isoconversional thermal analysis, activation energy, drug release, solid-state NMR

INTRODUCTION

In the last decade, there has been an increasing trend in isolating and evaluating polysaccharide-based hydrogels exuded from plant seed coats for potential applications in the medicinal and pharmaceutical fields.^{1,2} Water-swelling polysaccharide-based hydrogels have versatile characteristics, such as swelling, porous surface morphology, viscoelastic gelling nature and controlled permeability to small molecules and liquids with various pH, *etc.*^{3–5} Such naturally

occurring hydrogel possess swelling and deswelling properties in response to multiple external stimuli, such as pH, solvents and electrolyte stress.⁶ Furthermore, naturally occurring polysaccharide-based hydrogels have many advantageous properties over other biomaterials, as they are superporous, superabsorbent, biocompatible and biodegradable.^{7,8} Therefore, they could be potential candidates for the design of tablet

formulations for the development of sustained-release drug delivery systems, wound healing, tissue engineering, injectable polymeric systems, *etc.*⁹⁻¹³

Salvia spinosa is a plant of the *Lamiaceae* family. Its seeds are commercially available and sold under the name of Tukhm-e-Kanocha. The seeds of *S. spinosa* are light brown in color and rounded in shape. The seed size is 32.5 mm, with the epicarp of 75 μm , mesocarp of 35 μm , endocarp of 100 μm , and sclereids lumen of 63 x 13 μm . The seeds are tasteless and release a chemically modifiable hydrogel upon soaking in deionized water.^{14,15}

Our literature survey revealed that, so far, no study has been reported on the isoconversional thermal analysis and degradation kinetics of hydrogels from *S. spinosa* after acetylation. Acetylation is one of the valuable tools that direct to the development of some famous commercial products, such as cellulose acetate,¹⁶ starch acetate,¹⁷ dextran acetate,¹⁸ pullulan acetate,¹⁹ and acetate of linseeds with enhanced thermal stability, shelf life, and degradation kinetics.²⁰ These biomaterials, whether acetylated or not, are usually tested before use in various fields, especially in the pharmaceutical/medicinal industry. Seeking this connection, degradation profile and comparative isoconversional thermal analyses are applied to get information about their performance parameters, *i.e.*, use, storage and handling.^{21,22}

Hence, the main goal of our present research is to perform comparative isoconversional thermal analyses (Flynn-Wall-Ozawa (FWO) and Kissinger methods) of a polysaccharide-based hydrogel from *S. spinosa* (SSH) before and after acetylation (ASSH). The aim is to study the thermal stability (ITS, IPDT), kinetic triplets (E_a , n , A), and thermodynamic triplets (ΔG , ΔH , ΔS) of both SSH and ASSH. We are interested in evaluating the effect of increasing molar concentration of Ac_2O on the degree of acetylation onto the polymeric backbone of SSH. The aim is also the preliminary appraisal of the drug release behavior of the SSH-based matrix, with caffeine as a model drug.

EXPERIMENTAL

Materials

Salvia spinosa seeds were purchased from an indigenous marketplace of District Sargodha, Pakistan. All the reagents used in the study were obtained from Sigma-Aldrich.

Measurements

FTIR spectra of SSH and its acetylated derivatives were recorded on an IR Prestige-21 spectrophotometer (Shimadzu, Japan), using the KBr disc method. The solid-state NMR spectra of SSH and ASSH-4 were acquired using a CP/MAS ^{13}C -NMR (Bruker DRX-400) instrument at ambient temperature. The thermal degradation profiles of SSH and ASSH-4 were recorded in the ramp mode at four different onset heating rates, *i.e.*, 10, 15, 20 and 25 $^\circ\text{C}/\text{min}$ from ambient temperature to 800 $^\circ\text{C}$, under inert nitrogen atmosphere on an SDT Q600 thermal analyzer, provided with Universal Analysis 2000 software version 4.2E (TA Instruments, USA). Drug (caffeine) release quantification was performed, using a UV-Vis spectrophotometer (UV-1600 Shimadzu, Germany) at a wavelength of 273 nm.

Isolation of hydrogel from *S. spinosa* seeds

The seeds of *S. spinosa* were manually cleaned and soaked in distilled water (1:25; seed/DW w/v) for 2.5 h at 50 $^\circ\text{C}$. The hydrogel (SSH) thus produced by *S. spinosa* seeds was isolated by placing swollen seeds in a cotton cloth and by gentle rubbing with a spatula. The SSH obtained was defatted with *n*-hexane thrice and dried in a vacuum oven and stored. The dried SSH was milled, ground, and passed through a mesh sieve (No. 60). The yield of SSH was found to be 7.35 g/100 g.

Synthesis of ASSH

The SSH was acetylated using acetic anhydride (Ac_2O ; an acetylating agent).²³ The SSH (2.0 g, 12.34 mmol) was suspended in DMAc (50 mL) and heated at 80 $^\circ\text{C}$ for 1 h under stirring to homogenize the reaction mixture. After 1 h, Ac_2O (148.02 mmol) was added, followed by the addition of DMAP as catalyst (0.1 g), and the reaction was continued for 6 h at 70 $^\circ\text{C}$. The acetylated derivatives (reaction mixtures) were precipitated in methanol (250 mL). The precipitates of ASSH-4 were then isolated by filtration and further washed thrice with methanol (100 mL) to eliminate impurities.

Similarly, three more acetylated derivatives of SSH were synthesized using the varying concentration of Ac_2O , *i.e.*, 1:3 (ASSH-1), 1:6 (ASSH-2), and 1:9 (ASSH-3) and isolated via precipitation of the reaction mixtures in methanol, as indicated above. The DS of all the prepared samples were calculated by acidimetric titration after saponification in triplicate and the mean values are reported here. It was noted that the order of DS was the following: ASSH-4 > ASSH-3 > ASSH-2 > ASSH-1. Therefore, the sample ASSH-4 was further utilized for all of the thermal studies reported herein. Yield: 64% (ASSH-1); 73% (ASSH-2); 78% (ASSH-3); 83% (ASSH-4)
DS (Acidimetric titration): 1.05 (ASSH-1); 1.75 (ASSH-2); 2.20 (ASSH-3); 2.79 (ASSH-4)

FTIR (KBr), ASSH-1: 1736 (C=O ester), 1045 (C-O-C), 1414 (CH₂), 2899 (CH and CH₂), and 3154 (OH) cm⁻¹

FTIR (KBr), ASSH-2: 1742 (C=O ester), 1047 (C-O-C), 1450 (CH₂), 2868 (CH and CH₂), and 3321 (OH) cm⁻¹

FTIR (KBr), ASSH-3: 1737 (C=O ester), 1053 (C-O-C), 1422 (CH₂), 2909 (CH and CH₂), and 3280 (OH) cm⁻¹

FTIR (KBr), ASSH-4: 1744 (C=O ester), 1049 (C-O-C), 1431 (CH₂), 2914 (CH and CH₂), and 3304 (OH) cm⁻¹

Determination of degree of substitution (DS)

The DS of acetyl moieties onto SSH was calculated using a widely accepted acidimetric titration method, followed by saponification.^{24,25} ASSH-4 (0.1 g) was suspended in a NaOH (0.1M) aqueous solution overnight under stirring at 50 °C. The pH of the mixture was then maintained at 7 (neutral), using HCl (0.01M) and NaOH (1 M) solutions. The DS of SSH after acetylation was determined using Equation (1):

$$DS = \frac{[n NaOH \times M (RU)]}{[M_s - M_r (RCO) \times n NaOH]} \quad (1)$$

where $n.NaOH$ shows the number of moles of NaOH used after saponification, $M(RU)$ is the molar mass of the repeating unit of the polymer (anhydroglucose unit; AGU), M_s indicates the mass of sample used and $M_r(RCO)$ shows the molar mass of ester functionality.

Thermal analysis and degradation kinetics

The thermogravimetric (TG) and derivative thermogravimetric (DTG) curves recorded at the heating rate of 10 °C/min for both SSH and ASSH-4 (as a typical example) were used to calculate the thermal decomposition temperatures, such as initial (Td_i), maximum (Td_m), and final (Td_f) decomposition temperatures. The Flynn-Wall-Ozawa (FWO) method is the first isoconversional linear integral method. It was applied to the thermal degradation data and the values of kinetic and other thermal degradation parameters were calculated using Equation (2):²⁶⁻²⁸

$$\ln \beta = \frac{\ln A E_a}{R g(\alpha)} - 5.331 - 1.052 \frac{E_a}{RT} \quad (2)$$

where β represents the heating rate, A is a pre-exponential factor, E_a is the activation energy, R is a general gas constant, $g(\alpha)$ is equal to $\int_0^\alpha \frac{d\alpha}{f(\alpha)}$, T is the absolute temperature at the conversion rate (α).

Equation (3) helps to calculate the value of α :

$$\alpha = \frac{W_o - W_t}{W_o - W_f} \quad (3)$$

where W_o , W_f and W_t are the initial, final and sample mass (mg) at any temperature (T; K), respectively.

As the FWO method is based on the assumption that the rate of the thermal degradation reaction depends on the temperature at a fixed value of α , and is independent of any model that involves $g(\alpha)$ in the

integral form. Therefore, this method can also be termed as a model-free approach. So, a graph between the values of $\ln \beta$ along the ordinate (Y-axis) and $1000/T$ (K⁻¹) along the abscissa (X-axis) was plotted by fixing the value of α at multiple heating rates, resulting in a straight line. From the slope, the value of E_a was calculated and, from the intercept, the value of $\ln A$ was calculated.

Kissinger presented a method for the determination of the order (n) of the thermal degradation reaction. In this method, it was presumed that, in differential thermal analysis (DTA), the temperature of maximum deflection is the temperature at which the reaction rate is maximum. Equation (4) is used in this method:

$$\frac{\ln \beta}{(T_m)^2} = \frac{E_a}{RT_m} + C \quad (4)$$

At fixed values of α , a plot between $\log(\beta/T_m^2)$ vs. $1000/T_m^2$ furnishes the straight line.

Kissinger's method is also based on the ratio of tangential slopes of the second derivative thermogravimetric (2DTG) curve at right and left inflection points, *i.e.*, shape index (S). Equation (5) is used to calculate the value of S :

$$S = \frac{\left[\left(\frac{d^2 \alpha}{dt^2} \right) \right]_L}{\left[\left(\frac{d^2 \alpha}{dt^2} \right) \right]_R} \quad (5)$$

where subscript L indicates the thermal data on the left side of the 2DTG curve and subscript R indicates the thermal data on the right side of the 2DTG curve. The value of S is subsequently used to calculate the order of reaction (n) using Equations (6) and (7):

$$n = 1.88S \quad (S \geq 0.45) \quad (6)$$

$$n = 1.26S^{0.5} \quad (S \leq 0.45) \quad (7)$$

Determination of thermodynamic parameters of SSH and ASSH-4

The values of different thermodynamic parameters, such as Gibbs free energy (ΔG), enthalpy (ΔH) and entropy (ΔS) of SSH and ASSH-4 were calculated using the Eyring-Polanyi equation (Eqs. (8) and (9)):²⁹

$$k = \frac{k_B T}{h} e^{\frac{-\Delta G}{RT}} \quad (8)$$

$$\ln \frac{k}{T} = \frac{-\Delta H}{R} \times \frac{1}{T} + \ln \frac{k_B}{h} + \frac{\Delta S}{R} \quad (9)$$

where the parameters h and k_B are constants, representing Planck's and Boltzmann's constants, respectively.

The plot of the graph between $\ln k/T$ and $1/T$ gives a straight line with a slope and an intercept. From the slope, the values of ΔH can be determined, while from the intercept – those of ΔS for a given thermal degradation process; whereas the values of ΔG were calculated using Equation (10):

$$\Delta G = \Delta H - T\Delta S \quad (10)$$

The thermal stabilities of SSH and ASSH-4 were also assessed by calculating the values of integral procedural decomposition temperature (IPDT) and comprehensive index of intrinsic thermal stability (ITS) according to the Doyle method.³⁰ The Doyle method is more effective for the calculation of the values of IPDT and ITS as it involves the whole TG curve. These parameters were calculated from the TG curve obtained for all heating rates, by measuring the area under the curve; the mean of the values are reported here.

Evaluation of SSH as sustained-release material

Preparation of tablets

The sustained-release behavior of SSH was examined using caffeine as a model drug. Thus, SSH and caffeine-based oral tablet formulations (SSHC) were prepared using the already reported wet granulation method.³ Briefly, after passing through sieve no. 40, SSH (150 mg) and caffeine (100 mg) were mixed gently in a mortar and pestle. The obtained dry mixture was kneaded with a solution of PVP K30 (5% w/v in isopropyl alcohol) to get a damp mass. This damp mass was passed through sieve no. 20 to obtain uniformed size granules. Finally, the granules were dried in a hot air oven, lubricated with magnesium stearate (10 mg), and compressed into tablet form using a single punch machine fitted with flat surface stainless steel punches of 11 mm diameter. The tablets were prepared by maintaining the thickness and hardness in the ranges of 6-8 kg/cm² and 4.70-4.92 mm, respectively.

In vitro drug-release study

The *in vitro* release study of caffeine from SSHC was performed using USP Dissolution Apparatus II (Pharma Test, PT-DT7, Germany). The dissolution vessels were filled with buffers of pH 1.2, 6.8, and 7.4 (900 mL) by maintaining the temperature and paddle speed at 37 ± 0.5 °C and 50 rpm, respectively. An aliquot of the dissolution media was taken out after pre-defined time intervals and analyzed by a UV-Vis spectrophotometer at a wavelength of 273 nm (λ_{max} of caffeine). After each sampling, the level of the

dissolution media was replenished through a freshly prepared buffer of the respective pH.

Drug release mechanism

Drug release data were fitted by the zero-order kinetic (Eq. (11)) and Korsmeyer-Peppas model (Eq. (12)) to evaluate the drug release mechanism from SSHC tablets:

$$Q_t = K_0 t \quad (11)$$

$$\frac{M_t}{M_\infty} = k_p t^n \quad (12)$$

where Q_t represents the drug quantity at time t , and K_0 is the rate constant for the zero-order kinetic model. M_t/M_∞ denotes the quantity of caffeine released from SSHC at any time t . The k_p and n are the Korsmeyer-Peppas constant and diffusion exponent, respectively. From the value of n , the mechanism of drug release was determined. The mechanism followed Fickian diffusion ($n \leq 0.45$), non-Fickian diffusion ($0.45 < n < 0.89$), case-II transport ($n = 0.89$) and super case-II transport ($n > 0.89$).^{31,32}

RESULTS AND DISCUSSION

Synthesis and structure characterization

Acetylated derivatives of SSH were synthesized using different concentrations of acetic anhydride (Ac₂O) in DMAc as a solvent and DMAP as a catalyst. The SSH acetates (ASSH-1–4) were purified by re-precipitation and obtained as a colorless and powdery material with DS 1.05–2.79 of acetyl moieties. The products obtained were found soluble in DMSO, DMAc, and acetone, whereas insoluble in water, methanol and ethanol. The structures obtained were characterized by recording their FTIR and CP/MAS ¹³C-NMR spectra. The reaction conditions and results of acetylation of SSH are summarized in Table 1. The acetylation reaction is illustrated in Figure 1.

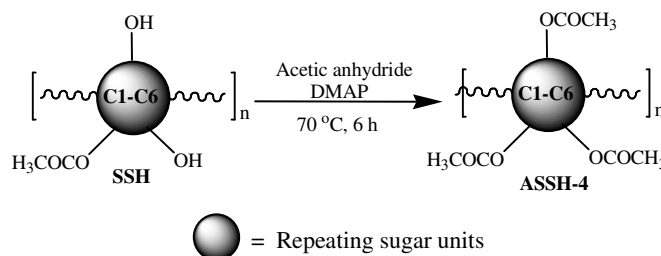


Figure 1: Schematic representation of acetylation of SSH

Table 1
Reaction conditions and results of acetylation of SSH (1.0 g)

| Sample | Molar ratio ^a | Yield (%) | DS ^b | Solubility |
|--------|--------------------------|-----------|-----------------|---------------------|
| ASSH-1 | 1:3 | 64 | 1.05 | DMSO, DMAc |
| ASSH-2 | 1:6 | 73 | 1.75 | DMSO, DMAc |
| ASSH-3 | 1:9 | 78 | 2.20 | DMSO, DMAc |
| ASSH-4 | 1:12 | 83 | 2.79 | DMSO, DMAc, acetone |

^aAnhydroglucose unit: acetic anhydride

^bDegree of substitution calculated by acid-base titration after saponification

FTIR spectroscopy

FTIR (KBr) spectra have indicated distinct ester peaks in acetylated samples (ASSH-1–4). Figure 2 shows the overlay spectra of SSH and ASSH-1–4. The appearance of peaks at 1736, 1742, 1737 and 1744 cm^{-1} in the spectra of ASSH-1, ASSH-2, ASSH-3 and ASSH-4, respectively, indicates the esterification of SSH. Signals of ester carbonyls and of the polymer backbone also appear in the

spectra. Additionally, it was also revealed that, by increasing the molar concentration of Ac_2O from 1:3 to 1:12, the DS also increased from 1.05 to 2.79. From the overlay FTIR spectra of ASSH-1–4, it can be accessed that the signal intensities of ester carbonyls are increasing and hydroxyls are decreasing as the molar ratios of acetic anhydride is increased from ASSH-1 to ASSH-4.

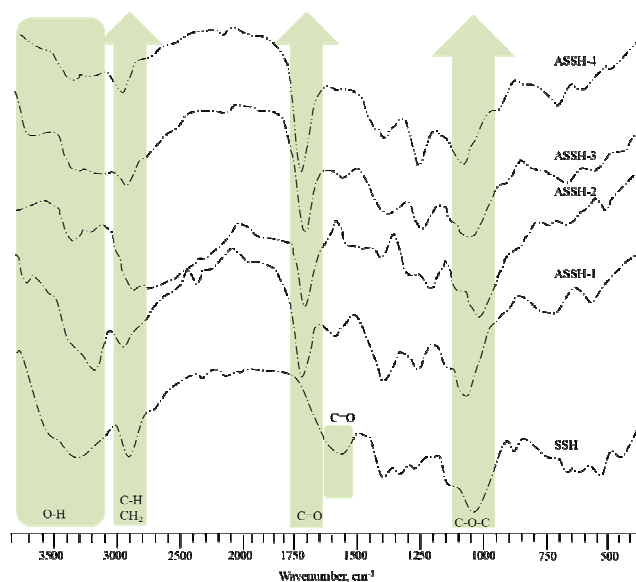


Figure 2: FTIR spectra of SSH and its acetylated derivatives ASSH-1–4

Solid-state CP/MAS ^{13}C NMR spectroscopic analysis

The solid-state CP/MAS ^{13}C NMR spectra of SSH (hydrogel) and acetylated SSH (ASSH-4) were recorded and shown in Figure 3 with the signal assignment. The spectrum of SSH showed a typical sugar pattern of the signals, which is comparable to another polyglucan polysaccharide. The signals at C-1 of glucans appear at 97.31 ppm, whereas overlapped signals for C-2-6 are seen in the solid-state NMR spectra at 55.15-

81.87 ppm. The spectrum of ASSH-4 showed a signal of carbonyl of acetate moieties at 162.81-168.90 ppm for ASSH-4. The C1, C2-6 peaks are labeled therein, showing the signals of repeating sugar units. It is also noted that traces of carbonyl from COOH groups, generally present in naturally occurring polysaccharide materials, showed their weak signals at 170 ppm in SSH. Such groups are responsible for the on-off switching of natural polysaccharides. Likewise, some methyl groups that are linked directly with the polymer backbone

(CH₃-C) are also present in traces and showed

signals at 25.46 ppm.

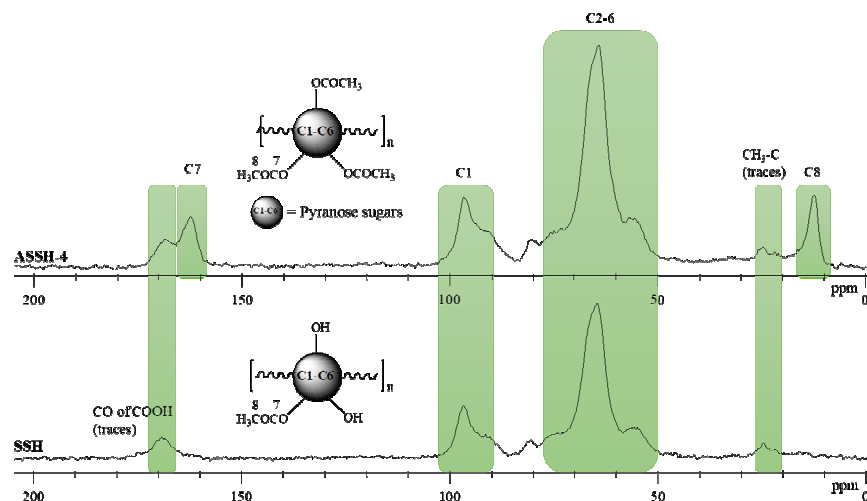


Figure 3: Solid-state CP/MAS ¹³C NMR spectra of SSH and ASSH-4

Thermogravimetric analysis

The thermal degradation data analysis of materials is an important step to acquire information about handling, storage, stability, shelf life, and some other material performance parameters, especially for pharmaceutical applications. Therefore, the thermal degradation behavior of SSH and ASSH-4 was evaluated by recording TG, DTG and 2DTG curves from ambient temperature to 800 °C, at multiple heating rates *i.e.*, 10, 15, 20, and 25 °C/min (Fig. 4a-f). It is obvious from the thermograms that both materials exhibited two-step thermal degradation. The values of thermal decomposition temperatures (Td_i, Td_f and Td_m) were calculated for each degradation step for both SSH and ASSH-4 from the DTG curve recorded at a heating rate of 10 °C/min and tabulated (Table 2). The Td_i for the first degradation step of ASSH-4 was found 27 °C greater than the Td_i of SSH;

likewise, the Td_m for the first degradation step of ASSH-4 was found 35 °C greater than the Td_m of SSH (see Table 2). Moreover, the Td_f of the first decomposition step of ASSH-4 was 15 °C greater than that of the first degradation step of SSH. Similarly, the Td_i, Td_m and Td_f of the second degradation step of ASSH-4 were found 15 °C, 15 °C, and 10 °C greater than the corresponding values of SSH, respectively (see Table 2). The mean value of IPDT was also calculated for ASSH-4 and SSH and found to be 451.0, and 388.53, respectively. These data show that extra stability was imparted to SSH after its conversion to its acetylated form (ASSH-4). For the sake of clarity regarding the thermal stability and the degradation profile of SSH and ASSH-4, overly TG and DGT curves of both materials were presented in Figure (5a, b), so it can easily understood that ASSH-4 is more thermally stable than SSH.

Table 2
Average thermal decomposition temperatures and char yield (%) of SSH and ASSH-4 at 10 °C/min heating rate

| Sample | Step | Td _i (°C) | Td _m (°C) | Td _f (°C) | Char yield (wt%) |
|--------|------|----------------------|----------------------|----------------------|------------------|
| SSH | I | 238 | 295 | 365 | 15.0 at 500 °C |
| | II | 385 | 415 | 480 | |
| ASSH-4 | I | 265 | 330 | 380 | 20.0 at 500 °C |
| | II | 400 | 430 | 490 | |

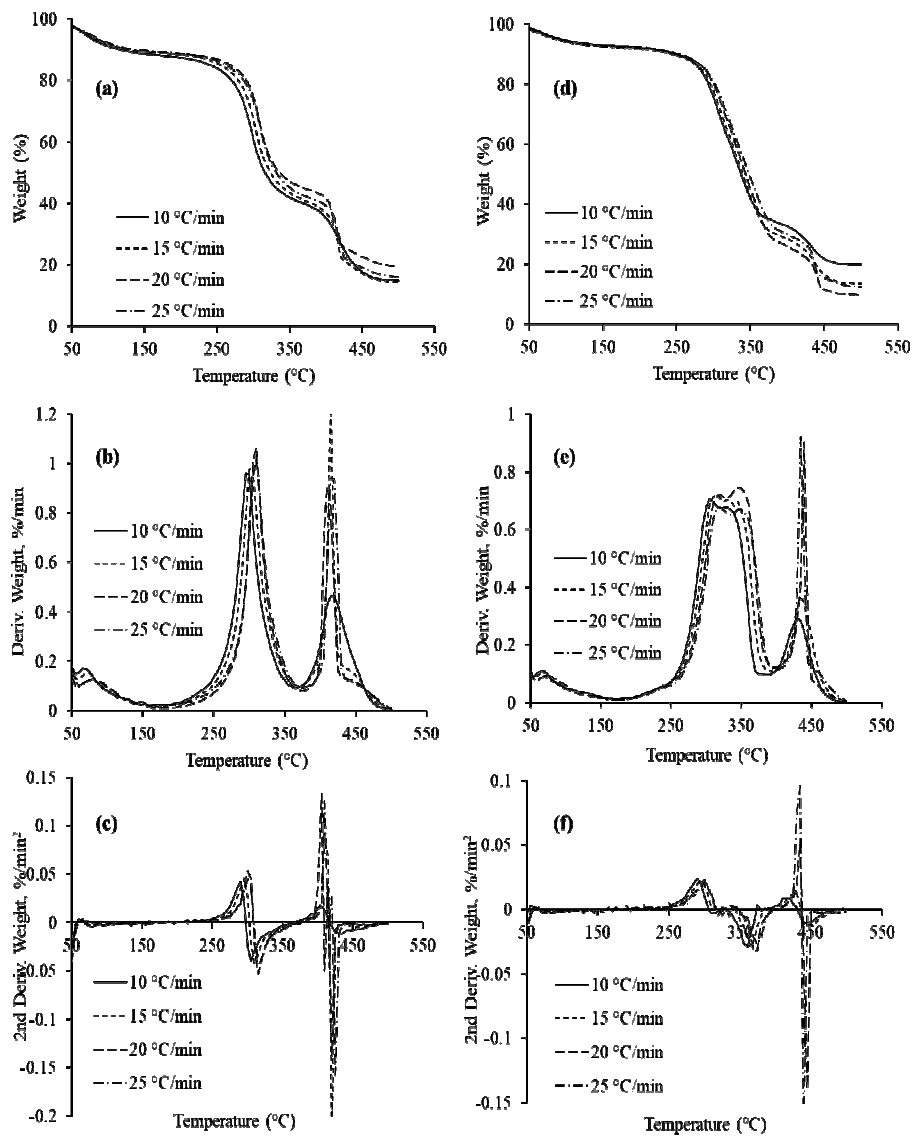


Figure 4: Overlay plots of TG, DTG and 2DTG curves of SSH (a-c), and ASSH-4 (d-f) at multiple heating rates

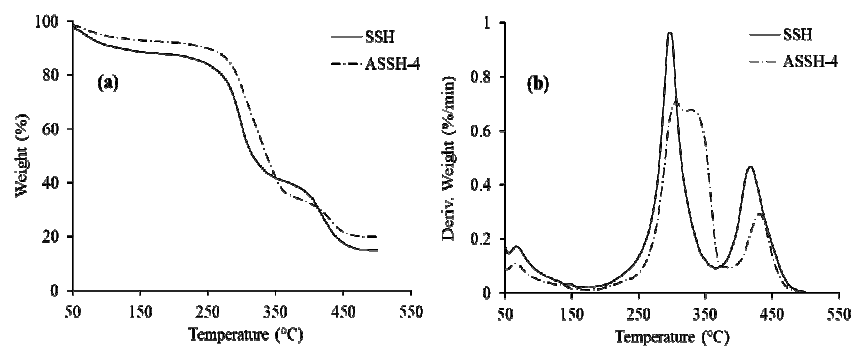


Figure 5: Overlay of TG (a) and DTG (b) curves of SSH and ASSH-4, showing comparative degradation profiles at a heating rate of 10 °C/min

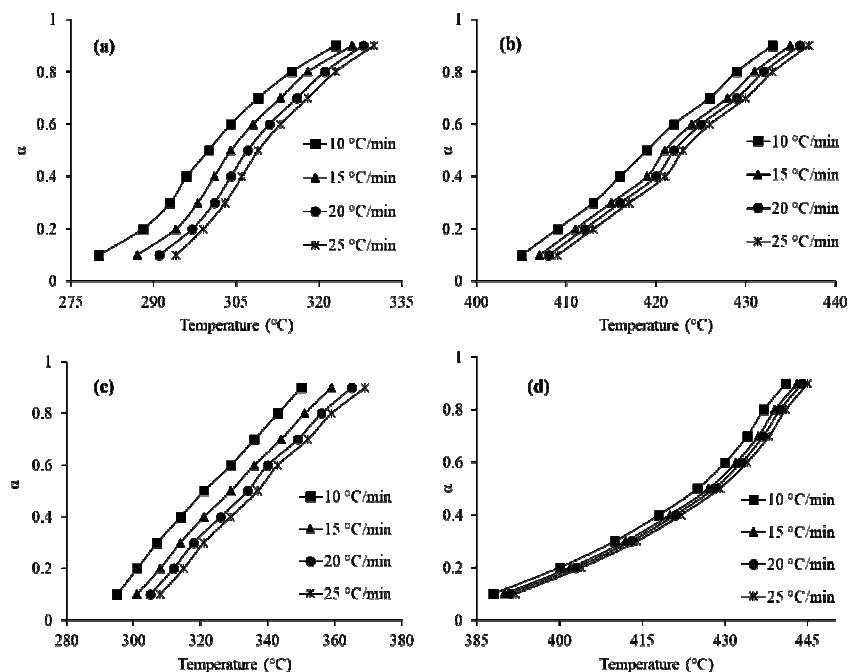


Figure 6: Plot of α vs. T curves of first (a, b) and second (c, d) thermal degradation steps of SSH and ASSH-4, respectively, at multiple heating rates

Degradation kinetics

The graph of α vs. T was plotted to study the influence of temperature on the conversion rate (α), at multiple heating rates, for each degradation step of SSH and ASSH-4 (Fig. 6a-d). The Flynn-Wall-Ozawa (FWO) model provides more authenticity in the determination of E_a at different values of the conversion rate ($\alpha = 0.1-0.9$ with 0.1 increments). Thereby, the FWO model was fitted to the TGA data obtained for the degradation step of both SSH and ASSH-4, to appraise the values of kinetic parameters, including E_a and frequency factor ($\ln A$). The straight-line plot between $\log \beta$ and $1000/T$ (K^{-1}) obtained from the FWO model of each degradation step for SSH and ASSH-4 is presented in Figure 7 (a, b and c, d, respectively). From the slope, the E_a values for SSH and ASSH-4 were calculated and found to be 180.2 and 202.7 kJ mol^{-1} , respectively, for the first degradation step, and 597.3 and 635.27 kJ mol^{-1} , respectively, for the second degradation step, which suggested a significant effect of acetylation on the rate of decomposition of SSH. Likewise, from the intercept of the plot, the values of $\ln A$ were calculated as 30.97 and 35.21 for the first degradation step, and 97.99 and 100.31 for the second degradation step (see Table 3).

The third kinetic triplet, *i.e.*, the order of decomposition (n), in each degradation step of SSH and ASSH-4 was calculated using the Kissinger method. The Kissinger plots of $\log(\beta/Tm^2)$ vs. $1000/Tm^2/K$ gave straight lines with correlation coefficients of 0.996 and 0.997 for the first and second decomposition steps of SSH, and of 0.999 and 0.997 for the first and second decomposition steps of ASSH-4, respectively (see Fig. 8a-d and Table 3). Herein, the T_{d_m} was taken as T_m , and calculated from the DTG curve recorded at a 10 $^{\circ}\text{C}/\text{min}$ heating rate. According to kinetic data, as calculated from the Kissinger model, the SSH showed second-order kinetics in both decomposition steps, Meanwhile, its acetylated derivative (ASSH-4) exhibited one and a half order kinetics in both thermal decomposition steps (Table 3). This can also be confirmed by carefully looking at the DTG curves of both SSH and ASSH-4 (see Fig. 5b). In the case of SSH, the curve is steep, while in the case of ASSH-4, the curve shows a relatively gradual weight loss with temperature. This indicates that the rate of decomposition of SSH is fast, as compared to that of ASSH-4. This is indicative of the fact that ASSH-4 can be favorably compared to SSH in terms of thermal stability.

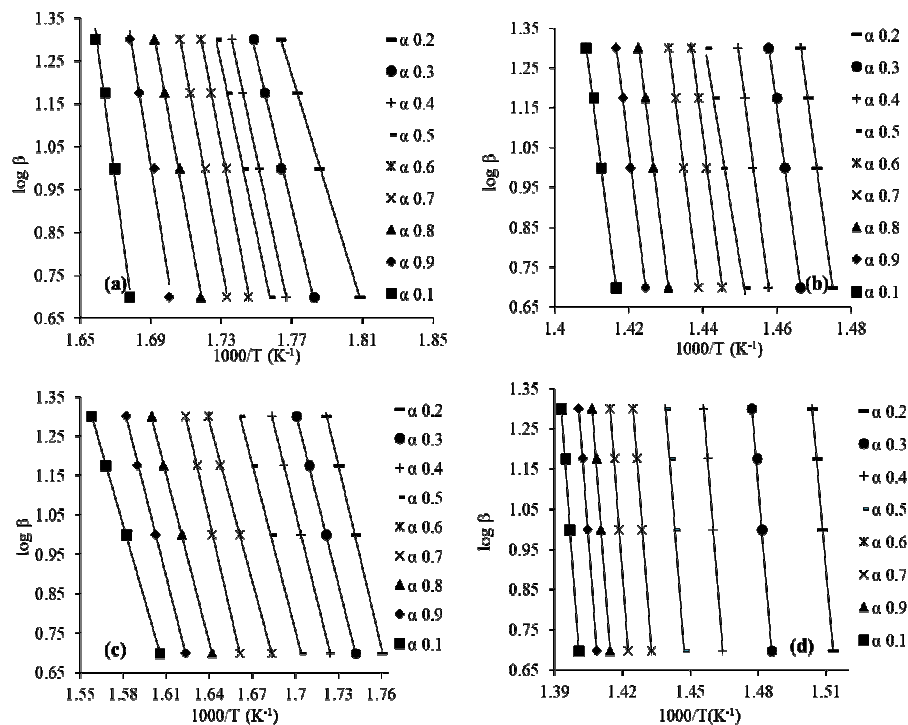


Figure 7: Plot of Flynn-Wall-Ozawa (FWO) method of $\log \beta$ vs. $1000/T$ (K^{-1}) for first (a, b) and second (c, d) degradation steps at several α values for SSH and ASSH-4, respectively

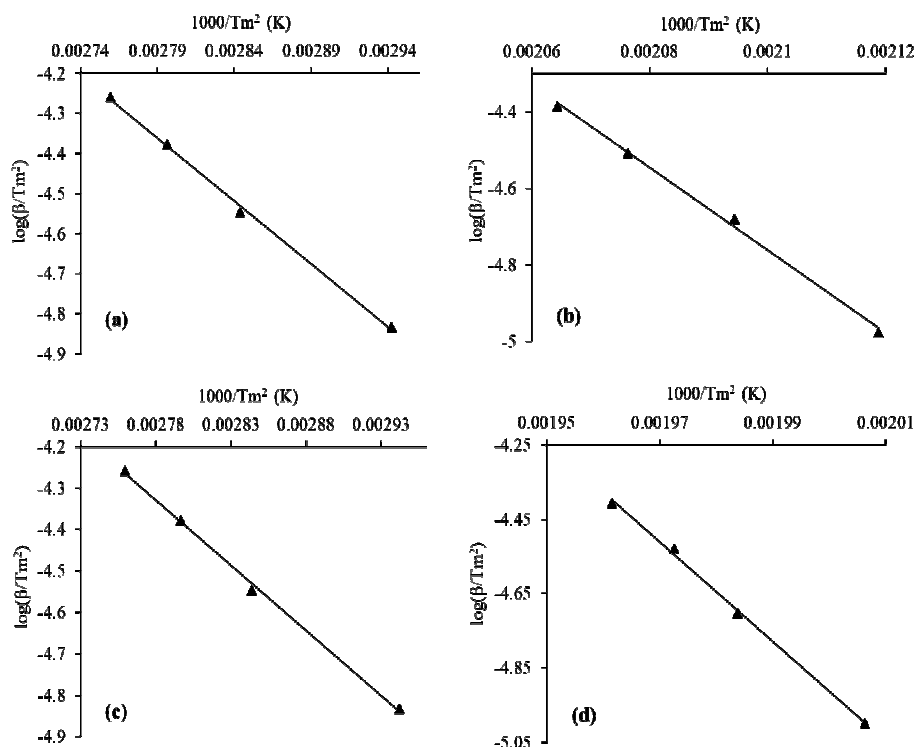


Figure 8: Plot of Kissinger method between $\ln(\beta/T_m^2)$ and $1000/T_m^2$ (K^{-1}) for first (a, b) and second (c, d) thermal degradation steps of SSH and ASSH-4, respectively

Table 3
Thermal kinetics and thermodynamic parameters of SSH and ASSH-4

| Sample | Method | Step | R^2 | n | E_a (kJ/mol) | $\ln A$ | ΔH (kJ/mol) | ΔS (J/mol/K) | ΔG (kJ/mol) | IPDT | ITS |
|--------|-----------|------|-------|------|-------------------|---------|------------------------|-------------------------|------------------------|--------|------|
| SSH | FWO | I | 0.996 | - | 180.2 | 30.97 | 175.4 | -873.41 | 679.2 | 388.53 | 0.50 |
| | Kissinger | I | - | 1.86 | - | - | - | - | - | | |
| | FWO | II | 0.997 | - | 597.3 | 97.99 | 591.6 | -317.75 | 809.92 | | |
| | Kissinger | II | - | 1.72 | - | - | - | - | - | | |
| ASSH-4 | FWO | I | 0.999 | - | 202.7 | 35.21 | 187.82 | -988.23 | 690.97 | 451.00 | 0.59 |
| | Kissinger | I | - | 1.58 | - | - | - | - | - | | |
| | FWO | II | 0.997 | - | 635.43 | 100.31 | 629.51 | -298.76 | 842.22 | | |
| | Kissinger | II | - | 1.50 | - | - | - | - | - | | |

Thermodynamic analysis

To evaluate the spontaneous or non-spontaneous nature of degradation of SSH and ASSH-4, the values of the thermodynamic triplet (ΔH , ΔG and ΔS) for SSH and ASSH-4 were calculated by putting the TG data of each of them in the Eyring-Polanyi equation (Eqs. 8 and 9; see Table 3). The positive values of ΔG and ΔH show the non-spontaneous nature of the degradation process. On the other hand, the negative values of ΔS show an orderly arrangement in the activated complex. The values of the thermodynamic triplets for ASSH-4 were found greater than those of SSH, which is indicative of stability imparted to the acetylated product, as compared to the unmodified SSH.

The values of ITS and IPDT were also calculated, as these values are very important in determining the thermal stabilities of the materials. To calculate these values, the area under the TG curves was calculated using Doyle's method.³⁰ For ASSH-4, the mean value of IPDT was found to be 451.0, and for SSH, the corresponding mean value of IPDT was 388.53. The mean values of ITS for SSH and ASSH-4 were found to be 0.50 and 0.59, respectively. Comparatively, greater values of IPDT and ITS for ASSH-4 than SSH revealed that ASSH-4 is thermally more stable than SSH. Moreover, the

values of ITS for SSH and ASSH-4 were also compared with those of other polysaccharide-based hydrogels isolated from plant seeds, such as *Salvia aegyptiaca* (0.33), *Argyrea speciosa* (0.35), *Astragalus gummifer* (0.38), *Plantago ovata* (0.39), *Acacia nilotica* (0.40), *Ocimum basilicum* (0.41), *Linum usitatissimum* (0.41), and *Mimosa pudica* (0.43), and were found to be higher, which reveals the higher stability of SSH and ASSH-4.^{20,33}

Drug release studies

The sustained release behavior of a model neutral drug (caffeine) from SSH and caffeine-based tablets (SSHC) was studied in the buffer of pH 1.2, 6.8 and 7.4 for 12 h (Fig. 9a). The cumulative drug release (%) from SSHC was found to increase as a function of pH as follows: pH 1.2 (20.1%) < pH 6.8 (96.7%) < pH 7.4 (99.0%) after 12 h. The drug release followed zero-order kinetics (Fig. 9b). The drug release mechanism was determined through the Korsmeyer-Peppas model, which indicated that the drug release followed the super case-II transport, *i.e.*, erosion base mechanism (Table 4). From this preliminary study, it can be established that SSH is an efficient material to design sustained and targeted release drug delivery systems.

Table 4
Mathematical data of zero order kinetics and Korsmeyer-Peppas model

| Formulation code | Dissolution medium | Zero-order | | | Korsmeyer-Peppas model | | | |
|------------------|--------------------|------------|-------|-------|------------------------|----------|-------|-------|
| | | R^2 | K_0 | MSC | R^2 | K_{KP} | n | MSC |
| SSHC | pH 6.8 | 0.9968 | 8.204 | 4.167 | 0.9945 | 6.424 | 1.110 | 4.862 |
| | pH 7.4 | 0.9969 | 9.050 | 4.401 | 0.9946 | 7.346 | 1.103 | 4.819 |

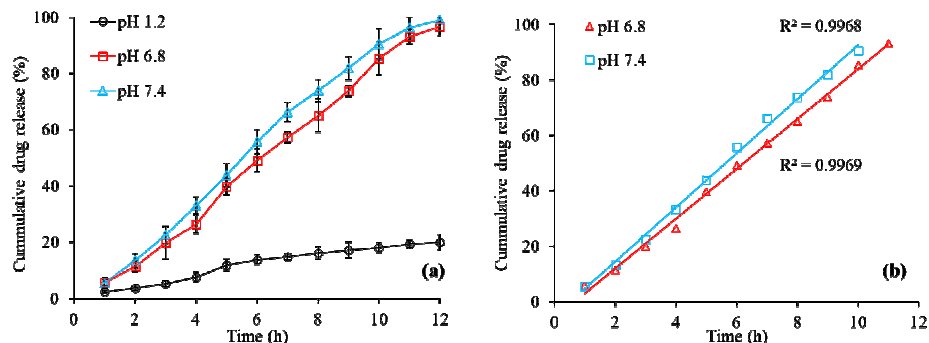


Figure 9: Release of caffeine from SSHC at pH 1.2, 6.8 and 7.4 (a), and release kinetics at pH 6.8 and 7.4 (b)

CONCLUSION

The *S. spinosa* hydrogel (SSH) is a modifiable material. The modified material (acetylated derivative ASSH-4) and unmodified SSH thermally decomposed in two steps, non-spontaneously, by following second-order kinetics. Concluding, it can be established that the stability of SSH is improved after acetylation and it can be recommended as a potential candidate to synthesize promising ester and ether derivatives with enhanced thermal stability. Preliminary results of caffeine release from the SSH-based matrix revealed the potential of SSH to be used as a future sustained release material for NSAIDs.

REFERENCES

- A. P. Galloway, P. Knox and K. Krause, *New Phytol.*, **225**, 1461 (2020), <https://doi.org/10.1111/nph.16144>
- E. Bakhshy, F. Zarinkamar and M. Nazari, *Int. J. Biol. Macromol.*, **137**, 286 (2019), <https://doi.org/10.1016/j.ijbiomac.2019.06.225>
- M. Farid-ul-Haq, M. A. Hussain, M. T. Haseeb, M. U. Ashraf, S. Z. Hussain *et al.*, *RSC Adv.*, **10**, 19832 (2020), <https://doi.org/10.1039/D0RA03176C>
- Z. Liu, W. Toh and T. Y. Ng, *Int. J. Appl. Mech.*, **7**, 1530001 (2015), <https://doi.org/10.1142/S1758825115300011>
- O. Liele and K. Ribbeck, *Trends Cell Biol.*, **21**, 543 (2011), <https://doi.org/10.1016/j.tcb.2011.06.002>
- M. Sabzi, M. J. Afshari, M. Babaahmadi and N. Shafagh, *Colloid. Surf. B: Biointerface*, **188**, 110757 (2020), <https://doi.org/10.1016/j.colsurfb.2019.110757>
- M. T. Haseeb, M. A. Hussain, S. H. Yuk, S. Bashir and M. Nauman, *Carbohydr. Polym.*, **136**, 750 (2016), <https://doi.org/10.1016/j.carbpol.2015.09.092>
- G. Muhammad, M. A. Hussain, M. U. Ashraf, M. T. Haseeb, S. Z. Hussain *et al.*, *RSC Adv.*, **6**, 23310 (2016), <https://doi.org/10.1039/C5RA23088H>
- S. Y. Yao, M. L. Shen, S. J. Li, X. D. Wu, M. M. Zhang *et al.*, *Colloid. Surf. B: Biointerface*, **186**, 110718 (2020), <https://doi.org/10.1016/j.colsurfb.2019.110718>
- J. S. Ribeiro, E. A. F. Bordini, J. A. Ferreira, L. Mei, N. Dubey *et al.*, *ACS Appl. Mater. Inter.*, **12**, 16006 (2016), <https://doi.org/10.1021/acsami.9b22964>
- P. Nezhad-Mokhtari, M. Akrami-Hasan-Kohal and M. Ghorbani, *Int. J. Biol. Macromol.*, **154**, 198 (2020), <https://doi.org/10.1016/j.ijbiomac.2020.03.112>
- Y. Ren, X. Yu, Z. Li, D. Liu and X. Xue, *J. Photochem. Photobiol. B, Biol.*, **202**, 111676 (2020), <https://doi.org/10.1016/j.jphotobiol.2019.111676>
- M. I. Sujan, S. D. Sarkar, S. Sultana, L. Bushra, R. Tareq *et al.*, *RSC Adv.*, **10**, 6213 (2020), <https://doi.org/10.1039/C9RA09528D>
- S. A. Oran, *Flora Mediterr.*, **7**, 27 (1997), <https://www.herbmedit.org/flora/7-027.pdf>
- A. Ali, M. A. Hussain, M. T. Haseeb, S. N. A. Bukhari, T. Tabassum *et al.*, *J. Drug Deliv. Sci. Technol.*, **69**, 103144 (2022), <https://doi.org/10.1016/j.jddst.2022.103144>
- J. Xu, Z. Wu, Q. Wu and Y. Kuang, *Carbohydr. Polym.*, **229**, 115553 (2020), <https://doi.org/10.1016/j.carbpol.2019.115553>
- D. Zhang, Z. Lin, W. Lei and G. Zhong, *Int. J. Biol. Macromol.*, **156**, 171 (2020), <https://doi.org/10.1016/j.ijbiomac.2020.03.256>
- M. Amin, M. A. Hussain, D. Shahwar and M. Hussain, *J. Chem. Soc. Pak.*, **37**, 673 (2015), <https://jcspp.org.pk/PublishedVersion/511ff214-015f-48d6-914c-f61a8fb46e45Manuscript%20no%207,%20Final%20Gally%20proof%20of%2010316%201MUHAMMAD%20AJAZ%20HUSSAIN.pdf>
- B. Preetam and S. Kale, *Adv. Sci. Eng. Med.*, **11**, 758 (2019), <https://doi.org/10.1166/ase.2019.2409>
- M. T. Haseeb, M. A. Hussain, S. H. Yuk, M. Amin, S. Bashir *et al.*, *Cellulose Chem. Technol.*, **52**, 681 (2018), [https://www.cellulosechemtechnol.ro/pdf/CCT7-8\(2018\)/p.681-688.pdf](https://www.cellulosechemtechnol.ro/pdf/CCT7-8(2018)/p.681-688.pdf)
- F. S. Felix, L. C. Cides da Silva, L. Angnes and J. R. Matos, *J. Therm. Anal. Calorim.*, **95**, 877 (2009), <https://doi.org/10.1007/s10973-007-8188-3>
- D. Giron, *J. Therm. Anal. Calorim.*, **68**, 335 (2002), <https://doi.org/10.1023/A:1016015113795>
- M. Amin, M. A. Hussain, S. A. B. Bukhari, M. Sher and Z. Shafiq, *Cellulose Chem. Technol.*, **51**, 245

(2017),

[http://www.cellulosechemtechnol.ro/pdf/CCT3-4\(2017\)/p.245-252.pdf](http://www.cellulosechemtechnol.ro/pdf/CCT3-4(2017)/p.245-252.pdf)

²⁴ M. A. Hussain, D. Shawar, M. Naeem-ul-Hassan, M. N. Tahir, M. S. Iqbal *et al.*, *Collect. Czech. Chem. Commun.*, **75**, 133 (2010), <https://doi.org/10.1135/cccc2009095>

²⁵ M. A. Hussain, D. Shawar, M. N. Tahir, M. Sher, M. Naeem-ul-Hassan *et al.*, *J. Serb. Chem. Soc.*, **75**, 165 (2010), <https://doi.org/10.2298/JSC1002165H>

²⁶ J. H. Flynn, *J. Therm. Anal. Calorim.*, **36**, 1579 (1990), <https://doi.org/10.1007/BF01914077>

²⁷ T. A. Ozawa, *Bull. Chem. Soc. Jpn.*, **38**, 1881 (1965), <https://doi.org/10.1246/BCSJ.38.1881>

²⁸ H. E. Kissinger, *Anal. Chem.*, **29**, 1702 (1957),

<https://doi.org/10.1021/ac60131a045>

²⁹ H. Eyring and M. Polanyi, *Z. Phys. Chem. Abt. B.*, **12**, 279 (1931)

³⁰ C. D. Doyle, *Anal. Chem.*, **33**, 77 (1961), <https://doi.org/10.1021/ac60169a022>

³¹ R. W. Korsmeyer, R. Gurny, E. Doelker, P. Buri and N. A. Peppas, *Int. J. Pharm.*, **15**, 25 (1983), [https://doi.org/10.1016/0378-5173\(83\)90064-9](https://doi.org/10.1016/0378-5173(83)90064-9)

³² P. L. Ritger and N. A. Peppas, *J. Control. Release*, **5**, 37 (1987), [https://doi.org/10.1016/0168-3659\(87\)90035-6](https://doi.org/10.1016/0168-3659(87)90035-6)

³³ M. S. Iqbal, S. Massey, J. Akbar, C. M. Ashraf and R. Masih, *Food Chem.*, **140**, 178 (2013), <https://doi.org/10.1016/j.foodchem.2013.02.047>